

## Linear and Nonlinear Polarizabilities of Fragmental Molecules for the Phenylacetylene Dendrimers

Yasushi Nomura,\* Takashi Sugishita, Susumu Narita, and Tai-ichi Shibuya

Department of Chemistry, Faculty of Textile Science and Technology, Shinshu University,  
Tokida 3-15-1, Ueda, Nagano 386-8567

(Received August 7, 2001)

Linear and nonlinear polarizabilities of small fragmental molecules for the phenylacetylene dendrimers have been calculated with the frequency-dependent moment schemes based on the sum-over-states expressions of the polarizabilities, including all of the singly-excited configurations in the semiempirical CNDO/S approximation. The smallest system, consisting of two benzene rings connected by an acetylene chain, corresponds to a molecular unit that is usually adopted in the exciton model for a theoretical analysis of the phenylacetylene dendrimers. The dependences of the polarizabilities upon the molecular size were examined. It has been shown that the linear polarizability in the static-field condition increases linearly with the number of acetylene chains ( $N$ ). MO calculations of the nonlinear polarizabilities of these molecules have been carried out for the first time. The third-order polarizability in the static-field condition is shown to depend quadratically upon  $N$ , which suggests that two chromophores at a time participate in the optical process of the third-order polarization.

Dendrimers consisting of a large number of hierarchically arranged molecular units<sup>1</sup> have attracted the attention of both chemists and physicists because of their unique structures and properties, including the optical response properties.<sup>2–17</sup> Phenylacetylene dendrimers have been most actively studied concerning their applicability to photon-harvesting devices in the visible-UV region.<sup>6–15</sup> They are classified into *compact* and *extended* dendrimers.<sup>7,9</sup> In the *compact* dendrimer, each benzene ring is connected at its *meta* positions to the neighboring benzene rings via an acetylene chain. On the other hand, in the *extended* dendrimer, the binding chains are lengthened toward the center by attaching  $-\text{C}_6\text{H}_4-\text{C}\equiv\text{C}-$ , where  $-\text{C}_6\text{H}_4-$  is the *para*-phenylene, although the *meta*-branching structure is the same as that in the *compact* dendrimer. Structures of small *compact* and *extended* dendrimers are schematically shown in Fig. 1. A phenomenon of the intramolecular energy transfer in the *extended* dendrimer was discovered by Devadoss et al.<sup>6</sup> and Shortreed et al.<sup>8</sup> in a perylene-terminated derivative, named “nanostar”. Many theoreticians investigated<sup>9–15</sup> the mechanism of this phenomenon, and showed that there existed an energy gradient toward the center of the *extended* dendrimer.<sup>9,11,12</sup> Moreover, using the exciton model, Kirkwood et al. analyzed the phenomenon in the time domain.<sup>15</sup>

While the mechanisms of energy transfers in dendrimeric systems have been actively investigated, the study of the nonlinear optical responses has only started.<sup>17</sup> For molecular aggregate systems, such as oligomers, however, the linear<sup>18–20</sup> and nonlinear<sup>21–29</sup> optical responses have been actively studied, and the frequency and the size dependences of the responses have been examined in detail, mostly with the exciton model.<sup>19–29</sup> For instance, Spano and Mukamel<sup>23</sup> showed that the third-order polarizability quadratically increased with the oligomer size under a long-wavelength condition. A dendrimer is

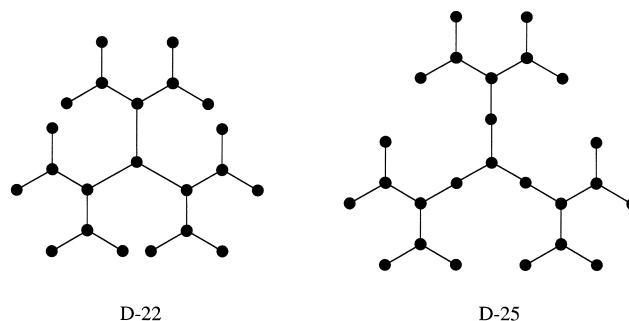


Fig. 1. Schematic representations of two types of phenylacetylene dendrimers: a *compact* dendrimer (D-22) and an *extended* dendrimer (D-25). In these figures, each dot denotes a benzene ring, and each line connecting two dots indicates an acetylene chain.

regarded as being a molecular aggregate system in which the constituent units are dendrimerically arranged. Therefore, it is interesting to study the optical responses of dendrimerically arranged aggregate systems. Because the number of molecular units in a dendrimer increases exponentially with the number of the branching generations, it is expected that the third-order polarizability may become extremely large for a higher branched dendrimer. From the viewpoint of developing efficient nonlinear optical media, it is therefore interesting to estimate the nonlinear polarizabilities of dendrimeric systems.

In this work, we calculated the linear and nonlinear polarizabilities of some molecular systems which are regarded as being parts of *compact* phenylacetylene dendrimers, based on the molecular orbital (MO) method, and investigated the dependences of the polarizabilities upon the molecular size. Taking into account a complete set of the singly-excited configura-

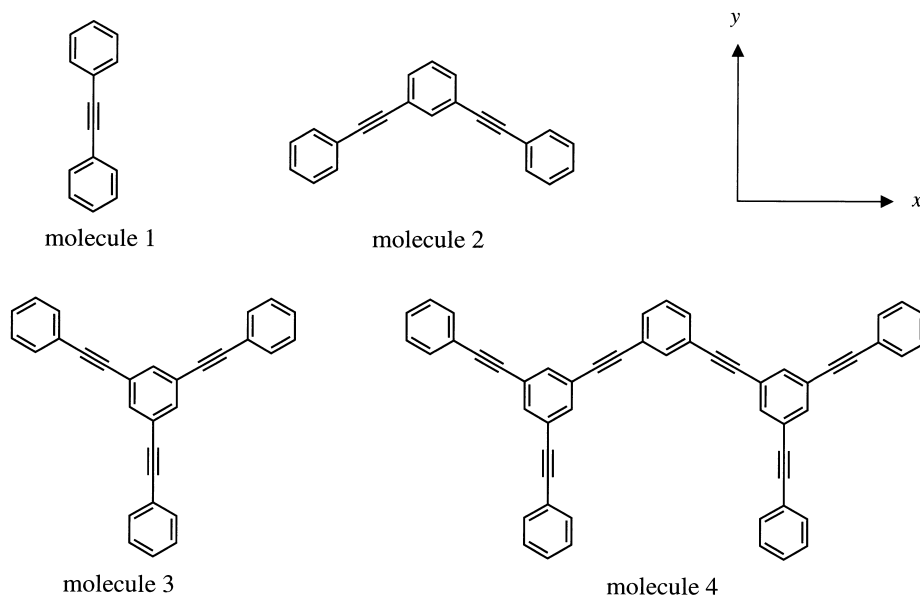


Fig. 2. Model molecules calculated in this paper. All take the planar structures, according to the geometry optimization in the AM1 approximation. The molecular planes are set in the  $xy$ -plane.

tions (SEC's), we evaluated the polarizabilities using the frequency-dependent moment (FDM) scheme proposed by Iwata<sup>30,31</sup> without diagonalizing the configuration interaction (CI) matrix. Previously, we confirmed that the scheme is useful to evaluate the molecular polarizabilities up to the third order,<sup>32</sup> and adopted the scheme to calculate the third-order polarizability of the C<sub>60</sub> molecule.<sup>33</sup> For the smallest system, consisting of two benzene rings connected by an acetylene chain, all of the eigensolutions of the CI matrix were used to examine the characteristics of the states contributing to the absorption peaks in the low-energy region.

### Calculation

The molecular systems discussed in this paper are shown in Fig. 2. They may be regarded as parts of *compact* phenylacetylene dendrimers. According to geometry optimization with MacSpartan<sup>34</sup> at the AM1<sup>35</sup> level, all of these molecules take planar structures, and molecules 1, 2, 3, and 4 belong to the point groups  $D_{2h}$ ,  $C_{2v}$ ,  $D_{3h}$ , and  $C_{2v}$ , respectively. We therefore set these molecular planes in the  $xy$ -plane, as shown in Fig. 2. In these optimized geometries, the C–C bond lengths are almost all the same at 1.4 Å, except for the triple bonds of 1.2 Å. While it has been pointed out that the dendrimer takes on a three-dimensional shape as the generation number increases,<sup>36</sup> the planar structures of these model molecules seem to be reasonable because the systems are rather small. The semiempirical CNDO/S<sup>37</sup> calculations were then carried out for these molecular systems. Full diagonalization of the CI matrix was carried out for molecule 1 in order to examine the characteristics of the electronic states contributing to the absorption peaks in the low-energy region. For other molecules, singly-excited configuration state functions were directly inputted in the FDM calculations of the polarizabilities. The FDM schemes are based on the sum-over-sum (SOS) expressions of the polarizabilities that are derived from the time-dependent perturbation theory (TDPT). According to the TDPT formulation by

Orr and Ward,<sup>38</sup> the SOS expressions of the first-, second- and third-order polarizabilities are written as

$$\alpha_{AB}(-\omega_\sigma; \omega_1) = \frac{1}{\hbar} \sum_P \sum_{n \neq g} \frac{\langle g | \hat{\mu}_A | n \rangle \langle n | \hat{\mu}_B | g \rangle}{\omega_{ng} - \omega_\sigma}, \quad (1)$$

$$\beta_{ABC}(-\omega_\sigma; \omega_1, \omega_2) = \frac{K(-\omega_\sigma; \omega_1, \omega_2)}{2! \hbar^2} \sum_P \sum_{n, m \neq g} \frac{\langle g | \hat{\mu}_A | m \rangle \langle m | \hat{\mu}_B | n \rangle \langle n | \hat{\mu}_C | g \rangle}{(\omega_{mg} - \omega_\sigma)(\omega_{ng} - \omega_2)}, \quad (2)$$

and

$$\gamma_{ABCD}(-\omega_\sigma; \omega_1, \omega_2, \omega_3) = \frac{K(-\omega_\sigma; \omega_1, \omega_2, \omega_3)}{3! \hbar^3} \times \sum_P \left\{ \sum_{k, m, n \neq g} \frac{\langle g | \hat{\mu}_A | m \rangle \langle m | \hat{\mu}_B | k \rangle \langle k | \hat{\mu}_C | n \rangle \langle n | \hat{\mu}_D | g \rangle}{(\omega_{mg} - \omega_\sigma)(\omega_{kg} - \omega_2 - \omega_3)(\omega_{ng} - \omega_3)} - \sum_{m, n \neq g} \frac{\langle g | \hat{\mu}_A | m \rangle \langle m | \hat{\mu}_B | g \rangle \langle g | \hat{\mu}_C | n \rangle \langle n | \hat{\mu}_D | g \rangle}{(\omega_{mg} - \omega_\sigma)(\omega_{ng} - \omega_3)(\omega_{ng} + \omega_2)} \right\}, \quad (3)$$

respectively, where the capital subscripts denote the Cartesian coordinates and  $\sum_P$  means a sum over the permutations of the pairs  $(-\omega_\sigma, \hat{\mu}_A)$  and  $(\omega_\ell, \hat{\mu}_\ell)$  in which  $\hat{\mu}_\ell = \hat{\mu}_B, \hat{\mu}_C, \hat{\mu}_D$  for  $\ell = 1, 2, 3$ , respectively. In Eqs. 2 and 3,  $\bar{\mu}_B$  is defined by  $\bar{\mu}_B = \hat{\mu}_B - \langle g | \hat{\mu}_B | g \rangle$ , where  $\hat{\mu}_B$  is the  $B$ -component of the electric dipole operator and  $|g\rangle$  the ground-state wave function. The induced polarization frequency ( $\omega_\sigma$ ) is related to the incident field frequencies ( $\omega_\ell$ ) by  $\omega_\sigma = \sum_\ell \omega_\ell$ .  $K(-\omega_\sigma; \omega_1, \omega_2)$  and  $K(-\omega_\sigma; \omega_1, \omega_2, \omega_3)$  in Eqs. 2 and 3 are numerical factors whose values depend upon the optical processes.

### Results and Discussion

**Linear Polarizability.** First, we examine the frequency

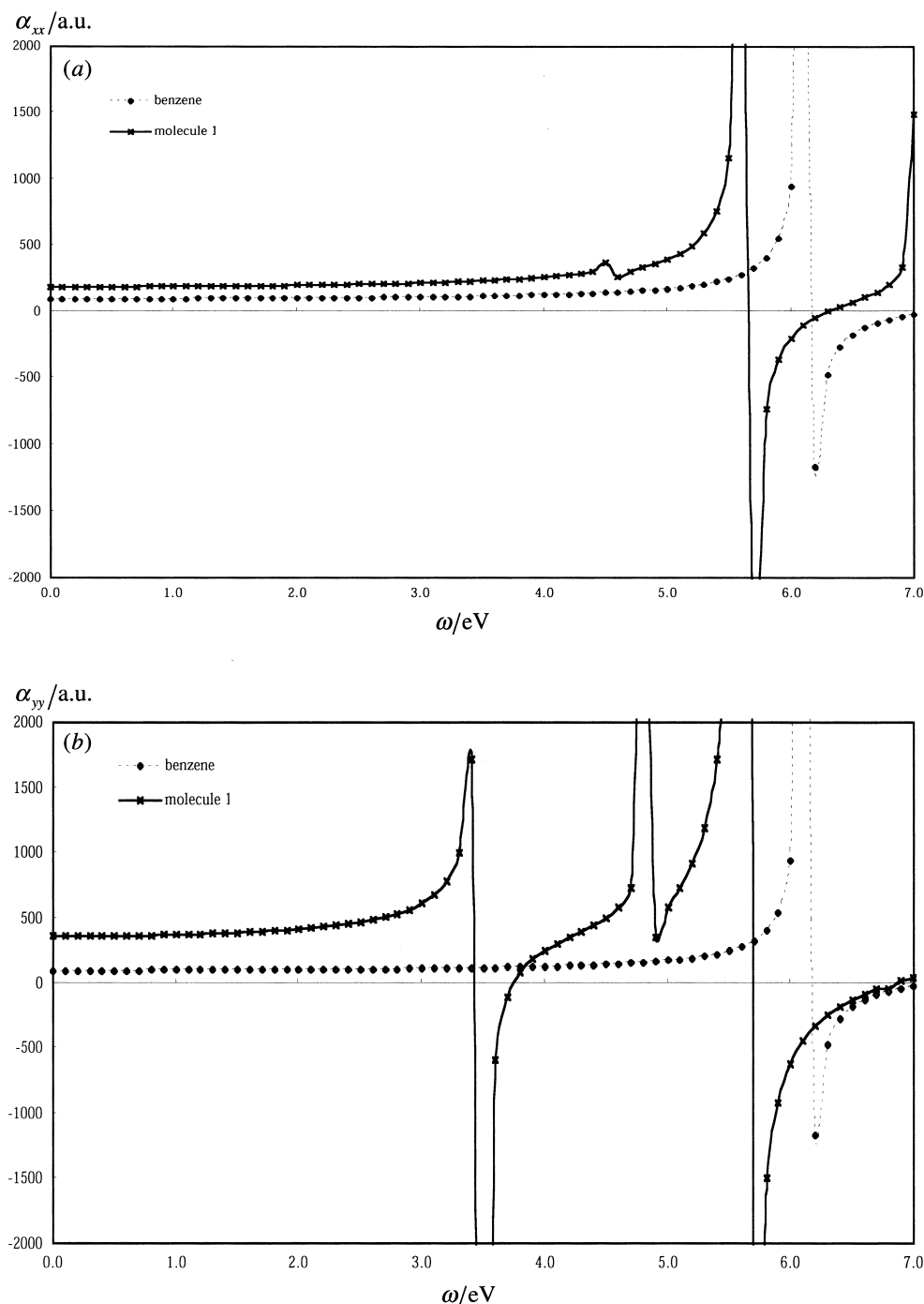


Fig. 3. Frequency dependences of the nonzero components  $\alpha_{xx}$  (a) and  $\alpha_{yy}$  (b), calculated for the molecule 1 (solid lines). Plots of the  $\alpha_{xx}$  and  $\alpha_{yy}$  of the benzene molecule are also shown (dashed lines) for comparison.

dependence of the linear polarizability of molecule 1. This molecule has been treated as a molecular unit in the exciton model for the phenylacetylene dendrimers.<sup>9–12</sup> The calculated values of the linear polarizability of the molecule 1 are plotted for the nonzero components,  $\alpha_{xx}$  and  $\alpha_{yy}$ , in Figs. 3a and 3b, respectively, as functions of the incident photon frequency. The calculated  $\alpha_{xx}$  and  $\alpha_{yy}$  values of the benzene molecule are also plotted for a comparison. The divergence points in Figs. 3a and 3b indicate the excitation energies of one-photon transition-allowed states (cf. Eq. 1); e.g., the points nearby 6 eV in

Figs. 3a and 3b for benzene correspond to the lowest  $^1E_{1u}$  state. The behaviors of the  $\alpha_{xx}$  and  $\alpha_{yy}$  of benzene are identical because the benzene molecule belongs to the  $D_{6h}$  point group. For molecule 1, which belongs to the  $D_{2h}$  point group, however, the behaviors of  $\alpha_{xx}$  along the lateral axis and  $\alpha_{yy}$  along the longitudinal axis are quite different. While the prominent lowest divergence point of  $\alpha_{xx}$  exists nearby 5.5 eV (Fig. 3a), the lowest divergence point of  $\alpha_{yy}$  appears at a much lower energy region nearby 3.5 eV (Fig. 3b).

By analyzing the eigensolutions of the CI matrix of mole-

cule 1, we can see that the state corresponding to the divergence point near 5.5 eV is dominantly due to the two SEC's,  $\text{HOMO} \rightarrow \text{LUMO} + 1$  and  $\text{HOMO} - 1 \rightarrow \text{LUMO}$ . We note that both  $\text{LUMO} + 1$  and  $\text{HOMO} - 1$  are practically localized at the two benzene rings and have a node along the acetylene chain. We also note that the shapes of these  $\text{LUMO} + 1$  and  $\text{HOMO} - 1$  at each benzene ring are very much like that of the HOMO and the LUMO of the benzene molecule, respectively. Thus, the transition near 5.5 eV originates considerably from the electronic transition localized at the benzene rings, and the corresponding state may be described in terms of the electronic states of the benzene molecule. On the other hand, the state corresponding to the divergence point near 3.5 eV in Fig. 3b is roughly assigned to the SEC of  $\text{HOMO} \rightarrow \text{LUMO}$ . We note that HOMO and LUMO are delocalized over molecule 1. Therefore, the state corresponding to the lowest divergence point reflects the characteristics of the  $\pi$ -conjugation extended over the molecule. From the absorption peak observed near 320 nm for the compact phenylacetylene dendrimer,<sup>7</sup> the excitation energy of the lowest transition-allowed state of molecule 1 was estimated to be about 3.9 eV. Although our calculated value 3.5 eV for the lowest state is slightly smaller, it may be essentially correct to say that the state is dominantly due to the  $\text{HOMO} \rightarrow \text{LUMO}$  excitation. Tretiak et al.<sup>9</sup> analyzed the localization/delocalization natures of these excited states using the INDO/S approximation, and derived the same conclusion.

Next, we consider the dependence of the linear polarizability upon the molecular size. Molecules 2, 3, and 4 show the lowest divergence at almost the same positions as that of molecule 1. This is expected from their *meta*-branching structures, in which the  $\pi$ -conjugation beyond the branching benzene ring is disrupted. Then, how does the intensity of the linear polarizability depend on the molecular size? Table 1 gives the nonzero components of the linear polarizabilities calculated in the static field condition for molecules 1, 2, 3, and 4. The values of the averaged polarizability, defined as  $\langle\alpha\rangle = (\alpha_{xx} + \alpha_{yy} + \alpha_{zz})/3$ , are also shown. The static field condition in this paper means that the incident photon energy is set to be equal to  $10^{-5}$  eV. We do so because the FDM calculation fails when the photon energy is strictly zero. This condition is reasonable because the linear and the nonlinear polarizabilities remain almost constant in the energy region near zero. The calculated values of  $\alpha_{xx}$ ,  $\alpha_{yy}$ , and  $\langle\alpha\rangle$  of the benzene molecule are also listed for a comparison. In Table 1, we notice that the  $\langle\alpha\rangle$  increases linearly with the number of acetylene chains. The number of acetylene chains corresponds to the number of mo-

Table 1. Nonzero Components and the Averaged Value of the Linear Polarizability (in a.u.) Calculated in the Static Field Condition

	$\alpha_{xx}$	$\alpha_{yy}$	$\langle\alpha\rangle$
molecule 1	185.4	359.1	181.5
molecule 2	557.6	355.7	304.4
molecule 3	645.4	645.4	430.3
molecule 4	1232.1	1232.1	803.7
benzene	93.7	93.7	62.5

lecular units in the exciton model.<sup>8-12</sup> The exciton model predicts the ratio of the  $\langle\alpha\rangle$  values relative to that of molecule 1 to be almost the same as the ratio of the numbers of units, i.e., 1:2:3:6. However, the ratio of our calculated values is 1:1.7:2.4:4.4. This ratio can be reproduced with a small error of around a few percent, using a simple equation,

$$\langle\alpha\rangle = N\langle\alpha_1\rangle - (N-1)\langle\alpha_0\rangle, \quad (4)$$

where  $\langle\alpha_1\rangle$  and  $\langle\alpha_0\rangle$  are the static values of molecule 1 and the benzene molecule, respectively, and  $N$  is the number of acetylene chains. If one sets  $\langle\alpha\rangle = N\langle\alpha_1\rangle$  for molecules 2, 3, and 4, as expected from the exciton model, the contributions of the benzene-originated states are overestimated for the branching benzene rings. The second term in Eq. 4 eliminates such overestimations. The additive property expressed in Eq. 4 suggests that the low-lying excited states of the phenylacetylene dendrimers can be described in terms of the excited states of the benzene molecule and the molecule 1.

**Second-Order Polarizability.** Table 2 shows nonzero components of the second-order polarizabilities for the second-harmonic generation process calculated in the static-field condition for molecule 2, 3, and 4. For molecule 1, the second-order polarizability vanishes because the molecule possesses the inversion symmetry. Although we were able to express the static linear polarizability by a simple formula in Eq. 4, the second-order polarizabilities of molecules 2, 3, and 4 can not be so easily estimated only from the excited states of the benzene molecule and molecule 1. A treatment taking into account only such states corresponds to the exciton model, in which the second-order polarizability vanishes for molecules 2, 3, and 4 because transitions between the ground state and the two-exciton states are then forbidden. It is therefore essential to include other types of excited states than just those of the benzene molecule and molecule 1 as the first or the second excited states.

**Third-Order Polarizability.** For all the planar systems lying in the  $xy$ -plane, as shown in Fig. 1, the nonzero components of the third-order polarizability in the static field condition are  $\gamma_{xxxx}$ ,  $\gamma_{xxyy} = \gamma_{xyxy} = \gamma_{yyxx} = \gamma_{yyxy} = \gamma_{yxyx} = \gamma_{yyxx}$ , and  $\gamma_{yyyy}$ . Components related to the  $z$ -axis vanish in the CNDO/S

Table 2. Nonzero Components of the Second-Order Polarizability (in a.u.) Calculated in the Static Field Condition

	$\beta_{xxy}$	$\beta_{xyx}$	$\beta_{yxx}$	$\beta_{yyy}$
molecule 2	-100.6	-100.6	-100.6	24.0
molecule 3	325.1	325.1	325.1	-325.1
molecule 4	466.2	466.2	466.2	-575.7

Table 3. Nonzero Components and the Averaged Value of the Third-Order Polarizability (in  $10^4$  a.u.) Calculated in the Static Field Condition

	$\gamma_{xxxx}$	$\gamma_{xxyy}$	$\gamma_{yyyy}$	$\langle\gamma\rangle$
molecule 1	-50.4	-42.4	-181.9	-63.4
molecule 2	-627.1	-97.5	-227.0	-209.8
molecule 3	-837.0	-279.0	-837.0	-446.4
molecule 4	-3550.4	-1099.5	-3069.4	-1763.8

approximation. Table 3 gives the components,  $\gamma_{xxxx}$ ,  $\gamma_{xyxy}$ , and  $\gamma_{yyyy}$  calculated for the third-harmonic generation process with the FDM scheme including all of the SEC's. The values of the averaged third-order polarizability, defined by

$$\langle \gamma \rangle = \frac{1}{5} \left[ \sum_{i=x,y,z} \gamma_{iiii} + \frac{1}{3} \sum_{i \neq j} (\gamma_{ijij} + \gamma_{ijji} + \gamma_{jiij}) \right], \quad (5)$$

are also shown. As can be seen in Table 3, these values are all negative. This is expected because only SEC's are included for the excited states. For linear polyene<sup>39</sup> and the C<sub>60</sub> molecule,<sup>33</sup> it has been pointed out that the static  $\langle \gamma \rangle$  values take negative values unless the doubly-excited configurations (DEC's) are taken into account. Referring to Eq. 3, we notice that the static  $\langle \gamma \rangle$  value becomes negative when the contribution of the second term in  $\Sigma_p$  is more dominant than that of the first one. Note that the absolute value of  $\langle \gamma \rangle$  shown in Table 3 increases steeply with the molecular size, i.e., 3.3, 7.0, and 27.8 for molecules 2, 3, and 4, respectively, relative to the value of molecule 1. These relative values vary between  $N(N+1)/2$  and  $N^2$ , where  $N$  is the number of acetylene chains. This  $N$ -dependence of  $\langle \gamma \rangle$  reflects the  $N$ -dependence of the second term in  $\Sigma_p$  of Eq. 3. As we have already seen in a discussion of the linear polarizability, the benzene molecule and molecule 1 act as chromophores in molecules 2, 3, and 4 in the low-energy region. Thus, the excited states  $|m\rangle$  and  $|n\rangle$  are approximately described in terms of singly-excited states of the chromophores. Because two sums over  $m$  and  $n$  in the second term of Eq. 3 are independent, two chromophores at a time participate in the optical processes of the third-order polarization, leading to a quadratic  $N$ -dependence.

Using the exciton model, Spano and Mukamel<sup>23</sup> analyzed the nonlinear optical responses of molecular aggregate systems, and showed that the third-order polarizability quadratically increased with the aggregate size in the long-wavelength condition. They clarified that the quadratic increase originated from two-exciton cooperations in the optical processes of the third-order polarization. In a two-exciton state of the coupled chromophore system, two chromophores are singly excited. Two-exciton states are generally described in terms of DEC's. Therefore, in order to investigate  $\langle \gamma \rangle$  more strictly, we will need a treatment that includes the DEC's.

### Summary

Taking into account all of the SEC's in the CNDO/S approximation, the FDM scheme has been applied to calculate the linear and nonlinear polarizabilities of some molecules, which are regarded as model systems for the compact phenylacetylene dendrimer. The nonlinear polarizabilities of these molecules have been evaluated for the first time based on the MO calculation. For the linear polarizability under the static-field condition, we have shown that the linear increase of the averaged  $\alpha$  with the number of the acetylene chains  $N$  is well described by Eq. 4. The additive property, as expressed in Eq. 4, suggests that transition-allowed states originating in the benzene molecule and molecule 1 dominantly contribute to the linear polarizabilities of molecules 2, 3, and 4 in the low-energy region. This indicates that these molecular parts act as chromophores for these molecules. For the third-order polarizability in the static field condition, we have shown that the ab-

solute value of  $\langle \gamma \rangle$  increases quadratically with  $N$ . The quadratic dependence suggests that two chromophores at a time participate in the optical processes of the third-order polarization. Hence, it is feasible to estimate the linear and third-order polarizabilities by regarding the whole molecules as aggregate systems consisting of chromophores. For the second-order polarizability, however, such a treatment fails because other types of excited states than those of the chromophores should participate as the first or the second intermediate states in the optical processes. Based on the MO calculation with the CNDO/S approximation, we have presented nonzero components of the second-order polarizabilities of molecule 2, 3, and 4.

### References

- 1 D. A. Tomalia, A. M. Naylor, and W. A. Goddard, *Angew. Chem., Int. Ed. Engl.*, **29**, 138 (1990).
- 2 D.-L. Jiang and T. Aida, *Nature*, **388**, 454 (1997).
- 3 A. Okada and H. Sumi, *Chem. Phys. Lett.*, **340**, 336 (2001).
- 4 Y. Nomura and T. Shibuya, *J. Phys. Soc. Jpn.*, **70**, 2205 (2001).
- 5 G. M. Stewart and M. A. Fox, *J. Am. Chem. Soc.*, **118**, 4354 (1996).
- 6 C. Devadoss, P. Bharathi, and J. S. Moore, *J. Am. Chem. Soc.*, **118**, 9635 (1996).
- 7 R. Kopelman, M. Shortreed, Z.-Y. Shi, W. Tan, Z. Xu, J. S. Moore, A. Bar-Haim, and J. Klafter, *Phys. Rev. Lett.*, **78**, 1239 (1997).
- 8 M. R. Shortreed, S. F. Swallen, Z.-Y. Shi, W. Tan, Z. Xu, C. Devadoss, J. S. Moore, and R. Kopelman, *J. Phys. Chem. B*, **101**, 6318 (1997).
- 9 S. Tretiak, V. Chernyak, and S. Mukamel, *J. Phys. Chem. B*, **102**, 3310 (1998).
- 10 E. Y. Poliakov, V. Chernyak, S. Tretiak, and S. Mukamel, *J. Chem. Phys.*, **110**, 8161 (1999).
- 11 K. Harigaya, *Phys. Chem. Chem. Phys.*, **1**, 1687 (1999).
- 12 M. Nakano, M. Takahara, H. Fujita, S. Kiribayashi, and K. Yamaguchi, *Chem. Phys. Lett.*, **249**, 323 (2000).
- 13 A. Bar-Haim, J. Klafter, and R. Kopelman, *J. Am. Chem. Soc.*, **119**, 6197 (1997).
- 14 A. Bar-Haim and J. Klafter, *J. Phys. Chem. B*, **102**, 1662 (1998).
- 15 J. C. Kirkwood, C. Scheurer, V. Chernyak, and S. Mukamel, *J. Chem. Phys.*, **114**, 2419 (2001).
- 16 O. Varnavski, A. Leanov, L. Liu, J. Takacs, and T. Goodson III, *J. Phys. Chem. B*, **104**, 179 (2000).
- 17 M. Nakano, H. Fujita, M. Takahata, and K. Yamaguchi, *J. Chem. Phys.*, **115**, 1052 (2001).
- 18 R. H. Lemberg, *Phys. Rev. A*, **2**, 883 (1970); **2**, 889 (1970).
- 19 S. Tretiak, V. Chernyak, and S. Mukamel, *J. Am. Chem. Soc.*, **119**, 11408 (1997).
- 20 S. Mukamel, S. Tretiak, T. Wagersreiter, and V. Chernyak, *Science*, **277**, 781 (1997).
- 21 F. C. Spano and S. Mukamel, *Phys. Rev. A*, **40**, 5783 (1989).
- 22 H. Ishihara and K. Cho, *Phys. Rev. B*, **42**, 1724 (1990).
- 23 F. C. Spano and S. Mukamel, *Phys. Rev. Lett.*, **66**, 1197 (1991).
- 24 F. C. Spano and S. Mukamel, *J. Chem. Phys.*, **95**, 7526 (1991).
- 25 J. Knoester, *Phys. Rev. A*, **47**, 2083 (1993).

- 26 S. Tretiak, V. Chernyak, and S. Mukamel, *J. Chem. Phys.*, **105**, 8914 (1996).
- 27 R.-H. Xie, *J. Chem. Phys.*, **108**, 3626 (1998).
- 28 M. Nakano and K. Yamaguchi, *Bull. Chem. Soc. Jpn.*, **71**, 1315 (1998).
- 29 M. Schulz, S. Tretiak, V. Chernyak, and S. Mukamel, *J. Am. Chem. Soc.*, **122**, 452 (2000).
- 30 S. Iwata, *Chem. Phys. Lett.*, **102**, 544 (1983).
- 31 T. Inoue and S. Iwata, *Chem. Phys. Lett.*, **167**, 566 (1990).
- 32 Y. Nomura, S. Miura, M. Fukunaga, S. Narita, and T. Shibuya, *J. Chem. Phys.*, **106**, 3243 (1997).
- 33 Y. Nomura, T. Miyamoto, T. Hara, S. Narita, and T. Shibuya, *J. Chem. Phys.*, **112**, 6603 (2000).
- 34 "Spartan ver. 5.0 programs for the Power Macintosh," Wavefunction, Inc., 18401 Von Karman, Suite 370, Irvine, CA 92612, USA.
- 35 M. J. S. Dewar, E. G. Zoebisch, E. F. Healy, and J. J. P. Stewart, *J. Am. Chem. Soc.*, **107**, 3902 (1985).
- 36 Z. Xu, M. Kahr, K. L. Walker, C. L. Wilkins, and J. S. Moore, *J. Am. Chem. Soc.*, **116**, 4537 (1994).
- 37 J. Del Bene and H. H. Jaffe, *J. Chem. Phys.*, **48**, 1807; 4050 (1968); **49**, 1221 (1968); **50**, 1126 (1969); R. L. Ellis, G. Kuehnlenz, and H. H. Jaffe, *Theoret. Chim. Acta*, **26**, 131 (1972).
- 38 B. J. Orr and J. F. Ward, *Mol. Phys.*, **20**, 513 (1971).
- 39 J. R. Heflin, K. Y. Wong, O. Zamani-Khamiri, and A. F. Garito, *Phys. Rev. B*, **38**, 1573 (1988).